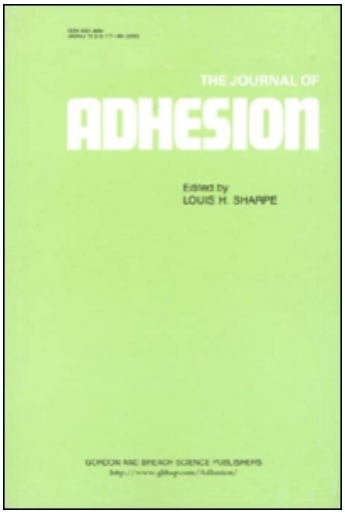

The Journal of Adhesion

Publication details, including instructions for authors and subscription information:
http://www.informaworld.com/smpp/title~content=t713453635

Interfacial Crack Propagation

D. R. Mulville[a]; R. N. Vaishnav[b]
[a] Ocean Technology Division, Naval Research Laboratory, Washington, D.C., U.S.A. [b] Department of Civil and Mechanical Engineering, The Catholic University of America, Washington, D.C., U.S.A.

To cite this Article Mulville, D. R. and Vaishnav, R. N.(1975) 'Interfacial Crack Propagation', The Journal of Adhesion, 7: 3, 215 — 233
To link to this Article: DOI: 10.1080/00218467508075052
URL: http://dx.doi.org/10.1080/00218467508075052

J. Adhesion, 1975, Vol. 7, pp. 215–233

Printed in Scotland

Interfacial Crack Propagation

D. R. MULVILLE

Ocean Technology Division, Naval Research Laboratory, Washington, D.C. 20375, U.S.A.

and

R. N. VAISHNAV

Department of Civil and Mechanical Engineering, The Catholic University of America, Washington, D.C. 20017, U.S.A.

(*Received January 15, 1975*)

Interfacial crack propagation studies were conducted on specimens of epoxy bonded to aluminum under both tensile and bending loads. The effect of surface roughness of the aluminum on fracture toughness was measured for four different surface finishes: polished, milled, glass-peened and sandblasted. It was found that increased surface roughness resulted in greater fracture toughness and that the interfacial cracks replicated the surface features of the aluminum. Microscopic studies of the failure surfaces indicated that crack propagation occurs in the epoxy near the interface, and that a residue of epxoy remains bonded to the aluminum. The magnitude of the residual stresses due to casting and curing of the epoxy was determined by photoelastic techniques. Methods were developed for analyzing the birefringent pattern in the epoxy to determine the magnitude of the elastic residual stress and the frozen stress. It was found that the residual stresses contributed 15 to 20% of the strain required for crack initiation at the interface.

1. INTRODUCTION

Due to their favorable strength and fabrication qualities, bonded joints and composite materials are finding increased use in aircraft and other modern engineering structures. Of particular importance in these applications are problems of debonding in joints and delamination in composites which in many cases limit their use to secondary structural members. Although considerable theoretical developments have been reported in the analysis of debonding and delamination problems, these problems have received limited experimental exploration. In this study the nature of the fracture process at interface of two bonded dissimilar materials is examined experimentally for bi-material specimens subjected to various loading conditions.

The plane problem of a crack between dissimilar materials was initially considered by Williams.[1] Using an eigenfunction approach, he analyzed the character of the stresses near the crack tip between two dissimilar isotropic materials joined without residual stress. He found that the resulting stresses possess an oscillatory character of the form $r^{-\frac{1}{2}} \sin(\lambda \log r)$ and $r^{-\frac{1}{2}} \cos(\lambda \log r)$, where r is the radial distance from the crack tip and λ is a function of material properties. This is in contrast to the homogeneous problem, in which the form of the resulting stresses near the crack tip is a $r^{-\frac{1}{2}}$ type of singularity.

Erdogan[2] considered a similar problem and obtained expressions for the stress along the bond in terms of complex potential functions. His results verify the oscillatory behaviour of the stresses previously described by Williams. In addition, he defined a pair of stress-intensity factors related to the Griffith–Irwin fracture theory. In the homogeneous problem, the stress-intensity factors, K_I and K_{II}, are associated with symmetric (normal) and skew-symmetric (shear) stress fields, respectively. However, for the non-homogeneous problem considered here, each of the stress-intensity factors is related to both symmetric and skew-symmetric stress fields. Later, Erdogan[3] analyzed the general plane problem of a series of through cracks along the interface subjected to known surface tractions and known dislocations in displacement along the bonded segments.

England[4] considered the plane problem of an internally pressurized crack between two dissimilar materials. He discussed the physical significance of the oscillatory behavior of the stresses and displacements near the crack tip. Mathematically, such oscillations implied that the upper and lower surfaces of the crack would have to wrinkle and overlap. England showed that these physically impossible interferences predicted by the analytic solution were confined to a very small region near the ends of the crack and he felt that on physical grounds the solution should provide a good approximation at points remote from this region. Rice and Sih[6] analyzed the problem of bending of a bi-material plate with cracks along the bond, and later, considered the general plane problem for interfacial cracks between dissimilar materials. Using a combination of the eigenfunction approach and the complex variable method, they formulated a solution for the stress and displacement fields and defined the stress-intensity factors in terms of a complex potential function.

While all of the preceding studies provided theoretical solutions to various types of interfacial problems for dissimilar materials, little experimental data was available to verify these results. Recently, Wu and Thomas[7] conducted an experimental study of crack propagation at the interface of a bi-material plate with loading normal to the bond. Using Rice and Sih's[6] analysis they determined the stress intensity factors for interfacial failure. The failure mode observed in their studies was a small amount of slow crack growth along the interface, followed by rapid crack propagation away from

the interface, leading to ultimate fracture. Wang[8] analyzed the plane problem of an interfacial crack between adhesively bonded dissimilar materials using numerical techniques. He also conducted an experimental compliance calibration to verify the results obtained in the numerical solutions. However, crack propagation studies were not conducted in his investigation.

Williams[9, 11] has conducted both analytic and experimental debonding studies using a pressurized blister test. This test was designed to treat the case of a soft elastomeric material cast, and cured on a relatively rigid substrate. A pressure inlet hole was drilled through the underside of the substrate, and pressure was applied which lifted the elastomeric layer off the surface of the substrate, forming a blister. This technique was applied by Burton, et al,[12] to study debonding of solid propellant and compatible liner from the rocket motor case. It has also been applied to measure the adhesive quality of dental cements, paints, explosively welded metal parts and barnacle cement. These applications are presented briefly in a recent paper by Bennett, *et al*,[13] in which he discusses the advantages and limitations of this test method. Its advantages are (1) ease of sample preparation, (2) ease of testing with relatively inexpensive equipment and (3) determination of several data points from a single specimen. However, for some materials, with a higher adhesive strength than cohesive strength, failure often begins at the periphery of the blister and extends into the material rather than along the bond.

The objective of this study was to examine in detail the nature of the fracture process at the interface of two bonded dissimilar materials by studying experimentally crack propagation in bi-material specimen subjected to a variety of loading conditions. Experimental studies were conducted for combinations of residual stresses, uniform thermal loading, external forces applied parallel to the bond and external moments which cause interfacial failure. A formulation was developed for the strain energy release rate, $\mathcal{G}$, for interfacial failure under these combinations of loads, Mulville.[14] For ease in illustrating the phenomena one of the materials in the example is considered as a relatively rigid body, i.e. the Young's modulus of one material is much greater than the other material.

THEORETICAL ANALYSIS

Consider two elastic half-spaces S^L and S^R as shown in Figure 1 with a common boundary, A, along the entire X axis; the positive Y axis being directed normally to the X axis, and lying wholly in S^L. Let the internal segment A' of the X axis bounded by the end points $(-l, 0)$ and $(l, 0)$ correspond to an interfacial bond with the remaining segment A'' on either side of A' representing two cracks. The total boundary A separating S^L and S^R is

the sum of A' and A''. Assume that each half-space is externally loaded by a system of self-equilibrating forces with A'' traction free. Under this loading there will be no resultant normal or shear forces transferred across A'. In addition, assume that the difference between the strains in S^L and S^R on A' is specified.

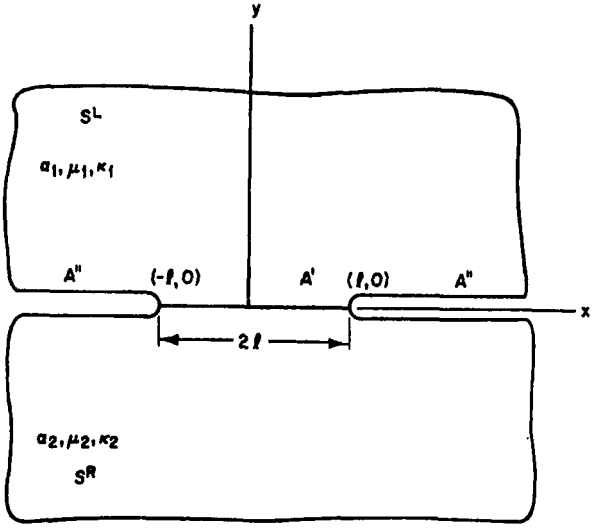

FIGURE 1 Two elastic half-spaces bonded along A'.

The boundary conditions can be expressed formally as follows: (1) the surface tractions vanish along the unbonded section of the real axis, A''; (2) the traction vector is continuous across A'; (3) the strain difference is specified on A'; (4) the components of the resultant force on A' are zero.

Using the complex potential function method as presented in Milne-Thomson,[15] the stress field was analyzed for the plane problem of two bonded dissimilar materials with cracks along the interface subjected to thermal loading or self-equilibrating tensile or bending loading applied to either half space. Each of the materials lying in S^L and S^R is assumed to be linearly elastic, homogeneous and isotropic. These results were used to formulate the strain energy release rate for crack propagation at the interface between the two materials. It should be noted that the resulting stresses obtained in this analysis possess an oscillatory character similar to that found by Williams.

The strain energy release rate, $\mathcal{G}$, defined as the decrease in stored elastic strain energy per unit of crack increase, was expressed as follows, Mulville, *et al.*[16]

$$\mathcal{G} = \frac{2\pi(1 + 4\lambda^2)}{a + b}\left[\eta^2 l - \frac{2\eta\lambda l^2}{R} + \frac{l^3}{4R^2}(1 + 4\lambda^2)\right] \tag{1}$$

where $a = \kappa_1/\mu_1 + 1/\mu_2$, $b = 1/\mu_1 + \kappa_2/\mu_2$, $c = a/b$ is defined as the bi-elastic constant, $\lambda = (\log c/2)\pi$ and

$$\eta = (\eta_R^L - \eta_R^R) + (\eta_T^L - \eta_T^R) + (\eta_M^L - \eta_M^R) \tag{2}$$

In Eq. (1) and (2), η_R is the strain due to residual stresses, η_T is the strain due to thermal loading, η_M is the strain due to mechanical loading, and R is the radius of curvature of A'. In the above μ_κ is the shear modulus, $\kappa_\kappa = (3\text{–}4\nu)$ for plane strain and $\kappa_\kappa = (3\text{–}\nu_\kappa)/(1+\nu_\kappa)$ for generalized plane stress, where ν_κ is Poisson's ratio.

The expression for the strain energy release rate is based on the plane problem of two elastic half spaces bonded along A', and can be used to analyze the following loading conditions; residual stresses, uniform thermal loading, self-equilibrating forces applied parallel to the bond to one or both half spaces, bending loads applied to one or both half space or any combinations of these loads. This analysis does not consider non-linear or viscoelastic effects, which may arise in bonding applications using polymeric adhesives. In addition, the strain function assumed along the bond in this analysis implies that one of the materials acts as a relatively rigid body, i.e. that the Young's modulus of one material is much greater than the other material. Otherwise, the resulting displacement on the interface must be considered an unknown function related to the material properties. This analysis also assumes that the crack growth will occur along the interface i.e. along $y = 0$.

EXPERIMENTAL INVESTIGATION

Experimental studies were undertaken to make quantitative measurements of the fracture parameter $\mathcal{G}$ for interfacial crack propagation. Using the analysis of the preceding section, specimen designs were chosen as shown in Figure 2, and loading conditions selected for which cracks would propagate at the interface between two dissimilar materials. In Figure 2, specimen thickness is 0.375 inches, $2l$ is the length of the bonded segment and m is the length of the initial cracks. Specimen design studies included photoelastic observations and strain gage instrumentation of these specimens to determine how closely the assumptions of the theoretical analysis were satisfied. Aluminum-epoxy specimens were then fabricated to conduct a series of interfacial crack propagation studies for various surface finishes on the aluminum surface of the bond. Restrained shrinkage along the bond during solidification of the epoxy and differential thermal contraction during post-curing gave rise to a field of residual stresses. The magnitude of these stresses was measured and their effect was included in the analysis.

The aluminum half of these specimens were 2×0.375 inch bar stock of 6061–T6 alloy. One of the 0.375 inch surfaces of each specimen was prepared

with one of four surface finishes, i.e. polished, milled, glass-peened or sand-blasted. The plates were cleaned and etched using methods similar to those currently used by the aircraft industry, DeLollis.[17] The etching process involved degreasing with tricloroethylene followed by immersion in a chromic-acid bath at 150 to 160°F for 10 minutes. The chromic acid bath consisted of a 30 : 10 : 1 by weight solution of distilled water, sulfuric acid and sodium dichromate. After etching the plates were rinsed in distilled water and

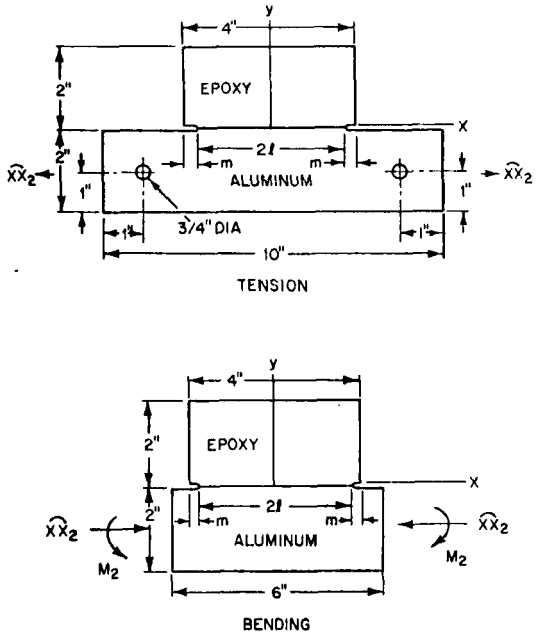

FIGURE 2 Specimen geometry for tension and bending specimens.

air dried. The aluminum plate was mounted in a mold with inserted teflon sides and end pieces, which were washed in detergent and air dried before casting of the epoxy. The epoxy consisted of 100 parts by weight of DER 332 epoxy resin and 12.5 parts by weight of tetraethylene pentamine hardener (TEPA). The mixture was heated to 110°F before casting to remove entrapped air bubbles and decrease viscosity. Solidification occurred in approximately 1 hour, and specimens were subsequently removed from the mold and post cured at 125°F for 4 hours. After post-curing, a saw cut was made in each end of the epoxy along the interface with a 0.020 inch thick blade. A razor blade was then used as a wedge to initiate a crack from the sawed notch. Dimensions of the epoxy plate were 2 inches in width × 4 inches in length × 0.375 inches in thickness. Values for the Young's modulus, E, and Poisson's

ratio, ν, for the aluminum were $E = 10^7$ psi and $\nu = 0.33$, experimentally measured values for the epoxy were $E = 5.7 \times 10^5$ psi and $\nu = 0.34$.

Bending loads were applied to aluminum plates as shown in Figure 3 at a rate of 500 lb/min, and the progress of interfacial failure was observed. Under this loading cracks propagated along the interface, and for bond lengths which were small with respect to other plate dimensions, the data could be analyzed using the techniques presented in the previous section.

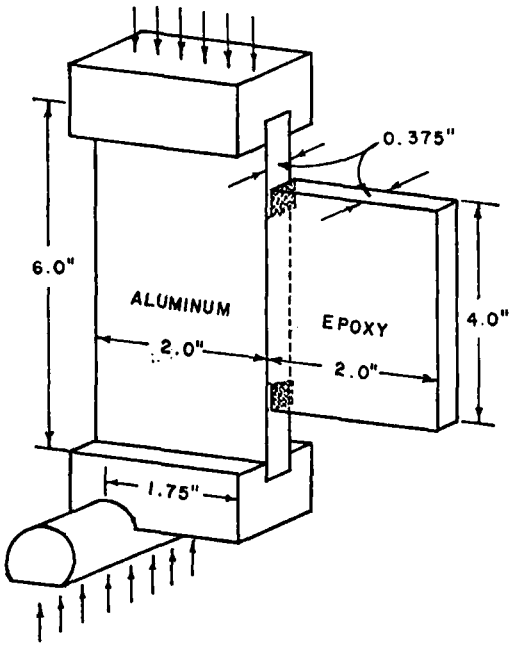

FIGURE 3 Specimen geometry and loading fixtures.

For this specimen, strain along the interface was determined from

$$\eta = \eta_M^L - \eta_M^R = \left(-\frac{y^L}{R^L} + \frac{y^R}{R^R}\right) + \left(\frac{XX_1}{E_1} - \frac{XX_2}{E_2}\right) \tag{3}$$

where, as shown in Figure 4, $y^L = y - h_e/2$ is the distance from the neutral axis of the epoxy plate of depth h_e, $y^R = y + h_a/2$ is the distance from the neutral axis of the aluminum plate of depth h_a, R^L and R^R are the radii of curvatures of the neutral axes, epoxy and aluminum respectively, due to flexure alone. This geometric description for bending analysis of two bonded plates follows closely the methods used by Boley and Weiner[18] for thermoelastic analysis of bending and buckling of bi-metallic beams. Evaluating this expression on A' corresponds to setting $y = 0$ in the relations for y^L and y^R

defined above. XX_1 and XX_2 are uniform stresses applied parallel to the bond in the epoxy and aluminum respectively and E_1 and E_2 are Young's moduli of the epoxy and aluminum respectively.

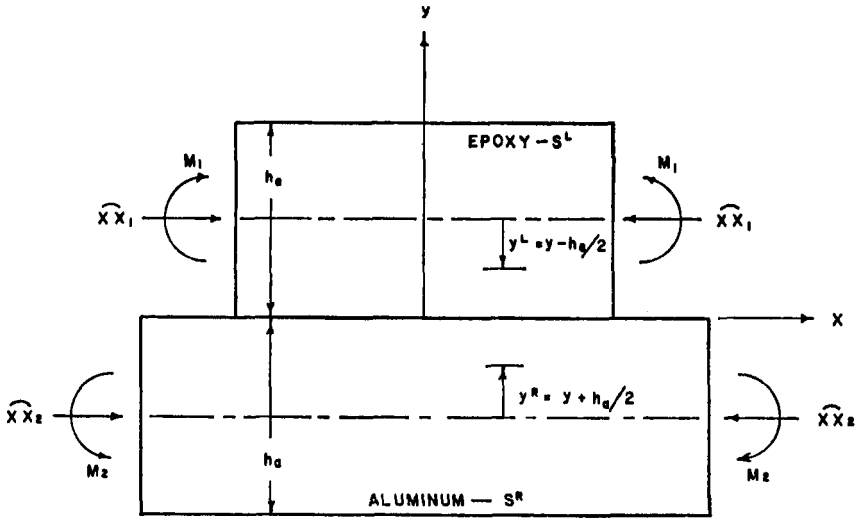

FIGURE 4 Plate specimen under self-equilibrating bending and compression loading.

Light field isochromatic fringe patterns are shown in Figure 5 for a bending specimen under progressively increasing load ($P = 9.4$ lbs). As shown in this figure, an increase in the applied load parallel to the bond resulted in an increase in the fringe order along the bond. Crack propagation occurred at a load of 3860 lbs which corresponds to a strain of 700 μin/in along the bond. It was relatively easy to follow the progress of the crack since the fringes approach the interface near the crack tip. Non-symmetric crack growth was observed in a number of these specimens. However, analysis of interfacial failure involves only the total bonded length and is unaffected by non-symmetric crack growth. Tensile loading was applied to the aluminum plates shown in Figure 2. Under this loading the cracks propagated along the interface, and, as in the case of the bending specimen, the strain was determined from Eq. (3). For both this specimen and the bending specimen the contribution due to bending loads was measured using strain gages bonded to the aluminum plates. Results of these experiments agree well with theoretical predictions of strain obtained from Eq. (3).

Light field isochromatic fringe patterns are shown in Figure 6 for a tensile specimen under progressively increasng load ($P = 18.8$ lbs). The fringe order at the interface increased as the load was applied up to approximately the

6th order at which time the crack began to propagate at the interface. For this specimen, crack initiation occurred at 7330 lbs, which corresponds to a strain of 1020 μin/in along the bond. To determine the total strain required for crack initiation, this value must be added to the strain due to the residual field.

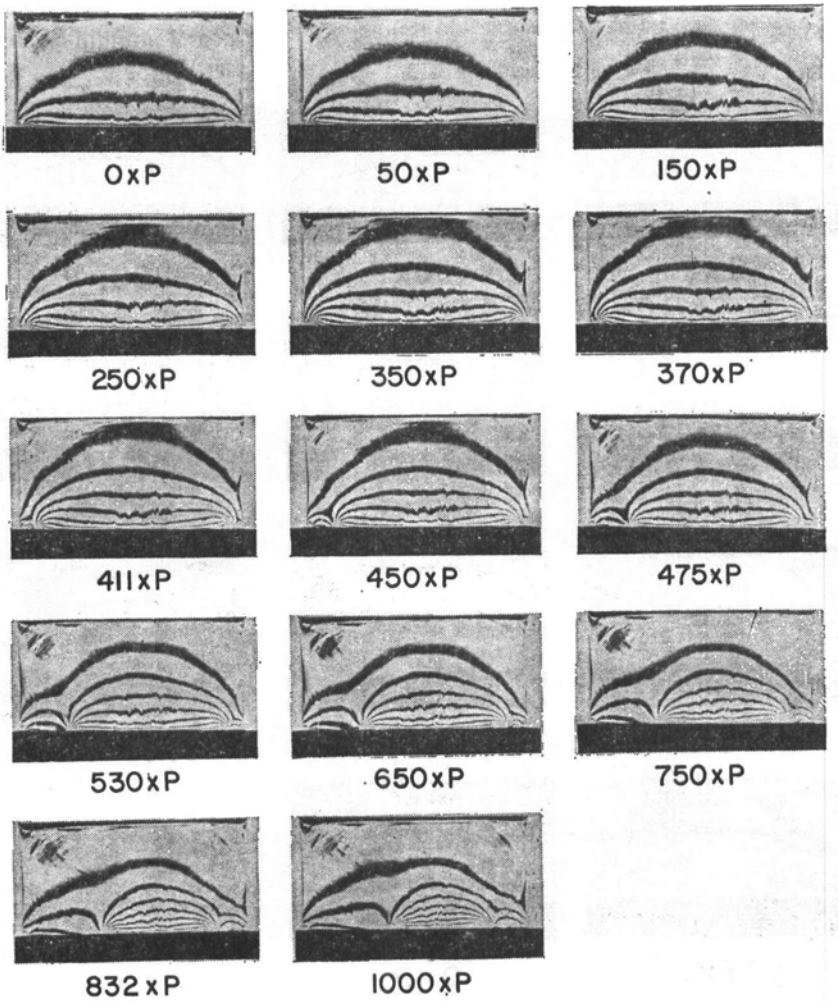

FIGURE 5 Isochromatic patterns for bonded plate under bending loads, $P = 9.4$ lbs.

Similar photoelastic patterns were obtained for an epoxy-aluminum bending specimen subjected to thermal loading alone. Crack propagation occurred when the specimen was reduced from room temperature, 75°F, to 10°F. This corresponds to a strain of approximately 1300 μin/in along the bond.

Variation in the measured value of the strain for crack initiation for these three studies, bending, tensile and thermal loading may be due to differences in the initial bond length, the magnitude of the residual field, and to difficulties associated with observation of initial crack growth.

A specimen of somewhat different design was used to determine the magnitude of the residual stress field induced due to casting and post-curing of the epoxy. This specimen was made by taking a $1 \times 1 \times 6$ inch aluminum bar and

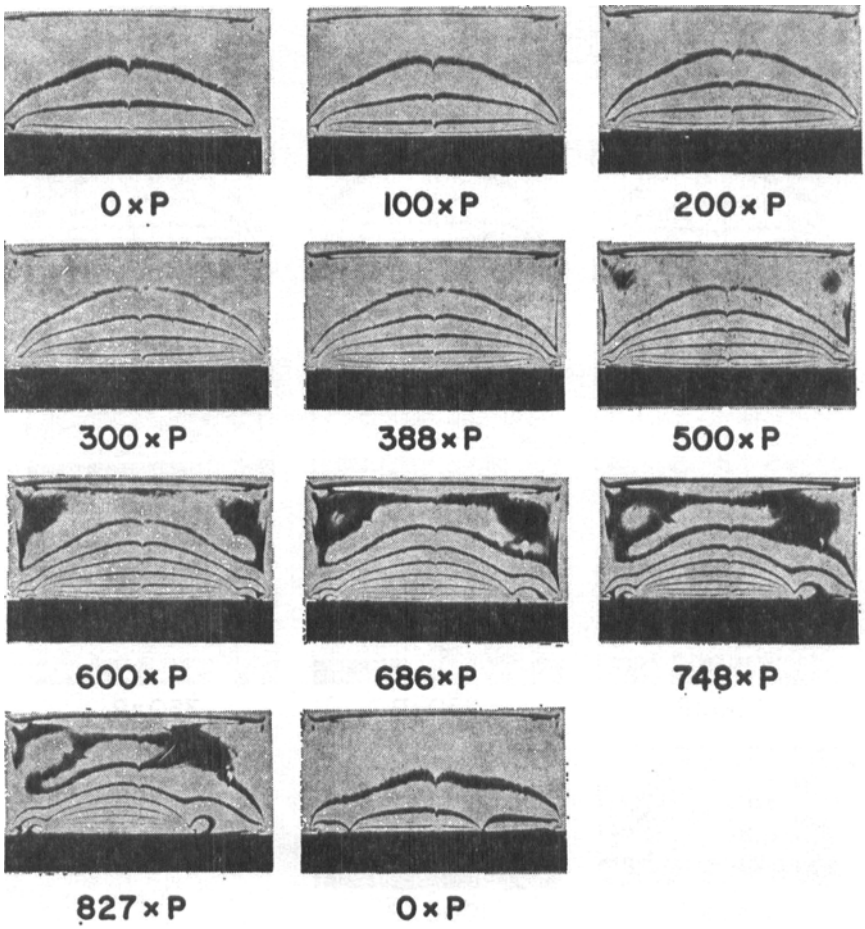

FIGURE 6 Isochromatic patterns for bonded plate under tensile loads, $P = 18.8$ lbs.

casting a $2 \times 4 \times \frac{3}{8}$ inch epoxy plate with a $4 \times \frac{3}{8}$ inch surface of the latter centrally located on a 1×6 inch aluminum surface. Compressive loads were then applied to the 1 inch square ends of the aluminum bar. Because of the difference in coefficient of thermal expansion of these materials and the

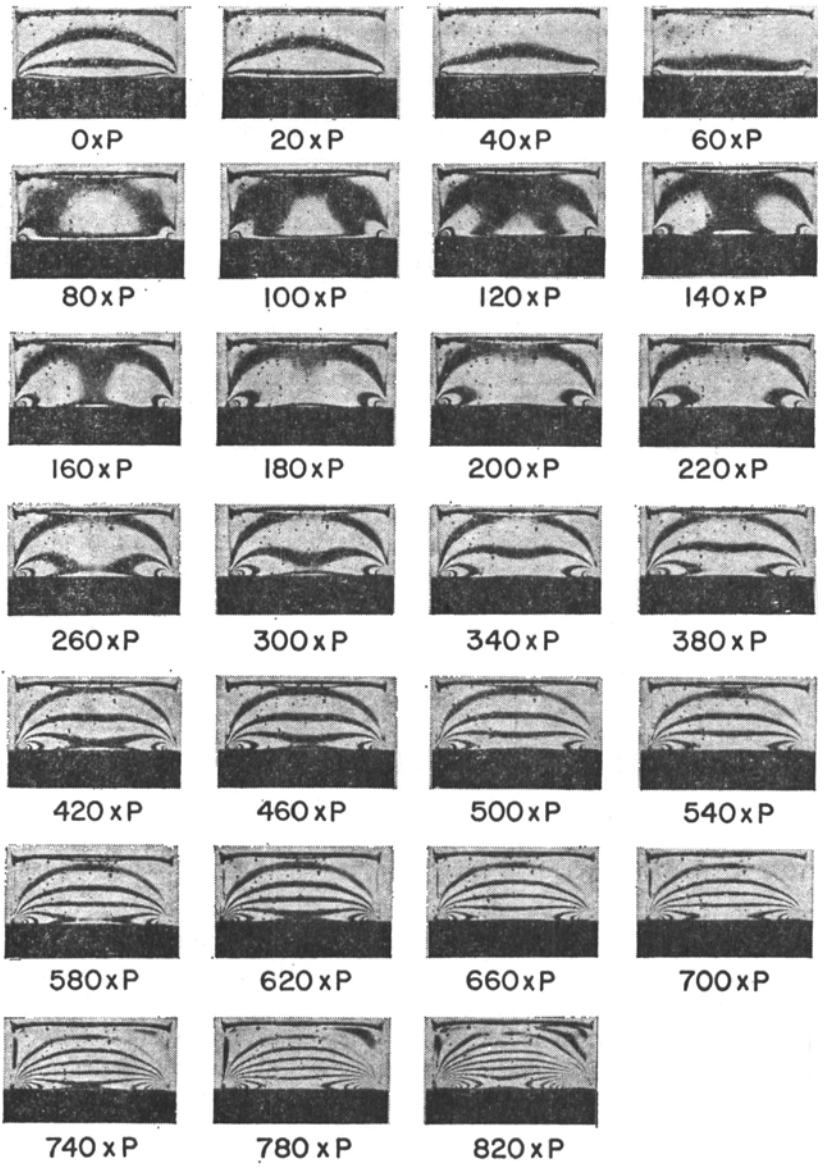

FIGURE 7 Isochromatic pattern for a bonded plate under compression loads, $P =$ 47.1 lbs.

elevated curing temperature, a tensile stress resulted in the epoxy when the specimen was returned to room temperature. Therefore, application of a compressive load to the aluminum parallel to the bond reduced the magnitude of the tensile residual stress. This was evidenced by a relaxation in the isochromatic pattern introduced during post-curing. Photographs of the light field isochromatic fringe patterns for the compression study are shown in Figure 7. Initial birefringence, as in the first frame of Figure 7, arose from two sources, elastic residual stresses and frozen stresses. The elastic stress field produced during the casting, post-curing and subsequent cooling process, stored elastic energy which was available for release to the fracture process. When the epoxy was debonded completely from the aluminum bar, birefringence due to the elastic stress field vanished, while birefringence due to the

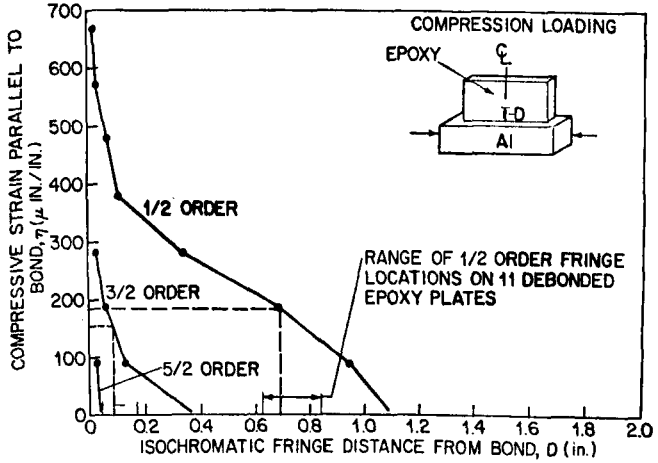

FIGURE 8 Strain *vs.* isochromatic fringe distance from bond for compression loading.

frozen stress field, which does not contribute to the fracture process, remained in the epoxy. To determine the magnitude of the elastic stress field, the position of the isochromatic fringes were measured along the center line perpendicular to the bond for various compressive loads applied to the aluminum bar. These results are shown in Figure 8. After crack propagation tests were completed on bending specimens, the epoxy was debonded and the position of the frozen isochromatic fringes was measured. The elastic strain required to produce an isochromatic pattern corresponding to the frozen isochromatic pattern was determined from Figure 8. Measurement of the position of the $\frac{1}{2}$ order fringe taken from the frozen isochromatic pattens from eleven specimens ranged from 0.62 to 0.84 inch. For these specimens the elastic strain due to residual stresses was 160 ± 30 μin/in. For the tensile specimen described above, the residual field contributed approximately 15% of the strain required

for crack initiation. This value was used in calculations of the energy required for crack propagation along the bond. For the compression specimen, crack propagation did not occur at the interface. Rather, the cracks deviated from the interface into the epoxy. This observation is in agreement with the theoretical analysis which predicts compressive normal stresses near the crack tip that may inhibit interfacial crack propagation.

RESULTS AND DISCUSSION

Using the formulation of the theoretical section, the strain energy release rate $\mathcal{G}$, was calculated at various crack lengths along the bond. This analysis is for two-dimensional bonded plates under either plane stress or plane strain conditions. In general, however, analysis of bonded plates is considered as a three-dimensional problem, since these plates experience a contraction in the thickness direction during curing or under mechanical

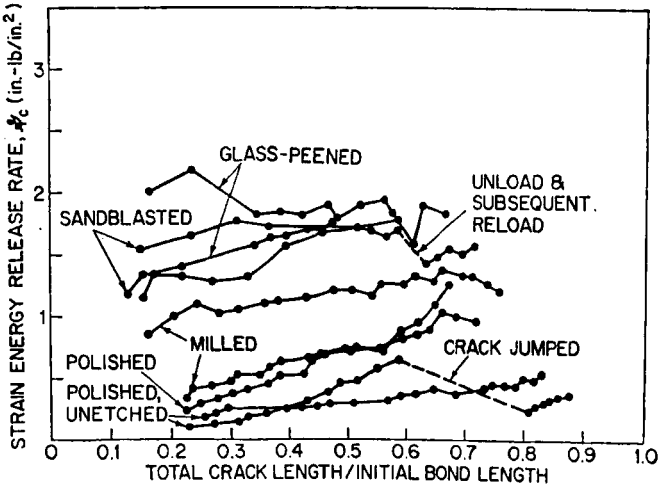

FIGURE 9 Strain energy release rate *vs.* crack length/initial bond length for various surface finishes on plates under bending loads.

loading. Durelli, *et al*[19] have shown that this pinching has little effect on the normal stress and strains along a bond for materials with similar Poisson's Ratio, and consequently, the two-dimensional analysis was considered adequate. Plane strain conditions were assumed in this analysis. From a physical point of view this is a reasonable assumption, since the aluminum constrains the epoxy at the interface. At regions remote from the interface, plane stress analysis may be more appropriate, since this constraint is no longer present.

Data shown in Figure 9 compares the results for bending tests on glass-peened, milled and sandblasted surfaces with polished aluminum surfaces. These values are generally greater than the value of $\mathcal{G} = 0.5$ in lb/in^2 for the bulk epoxy system reported by Mostovoy and Ripling[20]. However, for the polished specimens, the value of $\mathcal{G}$ are approximately equal to the bulk values. The crack velocities measured were fairly uniform and indicate relatively slow crack growth, approximately 3×10^{-3} in/sec. Therefore, the $\mathcal{G}$ values presented here can be taken as representative of these slow crack growth conditions. Milled, glass-peened and sandblasted surfaces were etched prior to casting of the epoxy. Specimens with polished surfaces were fabricated with both etched and unetched surface treatment. Results for tensile tests conducted on glass-peened and milled surfaces are similar to those presented for bending tests. Tensile tests on specimens with sandblasted surfaces indicate greater toughness than the bending specimens, although only limited studies have been completed. Insufficient data was obtained from the thermal loading studies to make valid comparisons with the results of the bending or tensile studies.

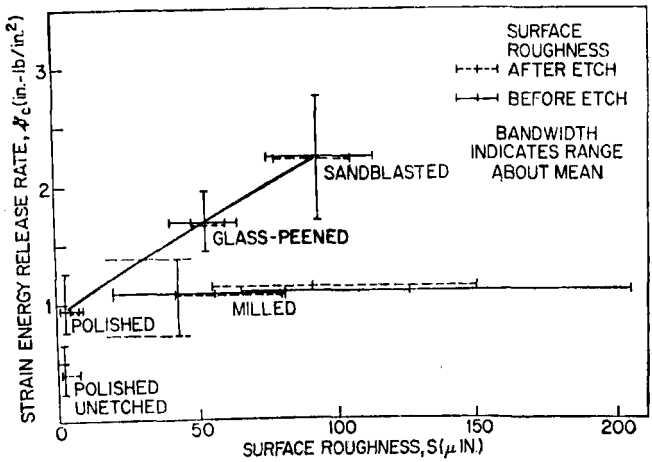

FIGURE 10 Strain energy release rate *vs.* surface roughness for specimens under bending loads.

Values of the surface roughness were measured for the various surface finishes, both before and after etching. Surface roughness measurements were made with a profilometer which draws a tracer point across the surface and indicates the arithmetic average of the roughness. The tracer point used for these measurements was conical with a hemispherical tip having a 0.0005 inch radius. Figure 10 shows that for polished, glass-peened and sandblasted surfaces, which were etched prior to casting and were subjected to bending

loading, there is a linear relation between surface roughness and strain energy release rate. This can be expressed as

$$\mathcal{G} = 0.014\ S + 0.9 \tag{4}$$

where S is the surface roughness in microinches measured using the method described above. These measurements indicate that the milled surface roughness is non-uniform, i.e. the surface roughness along the length of the bond

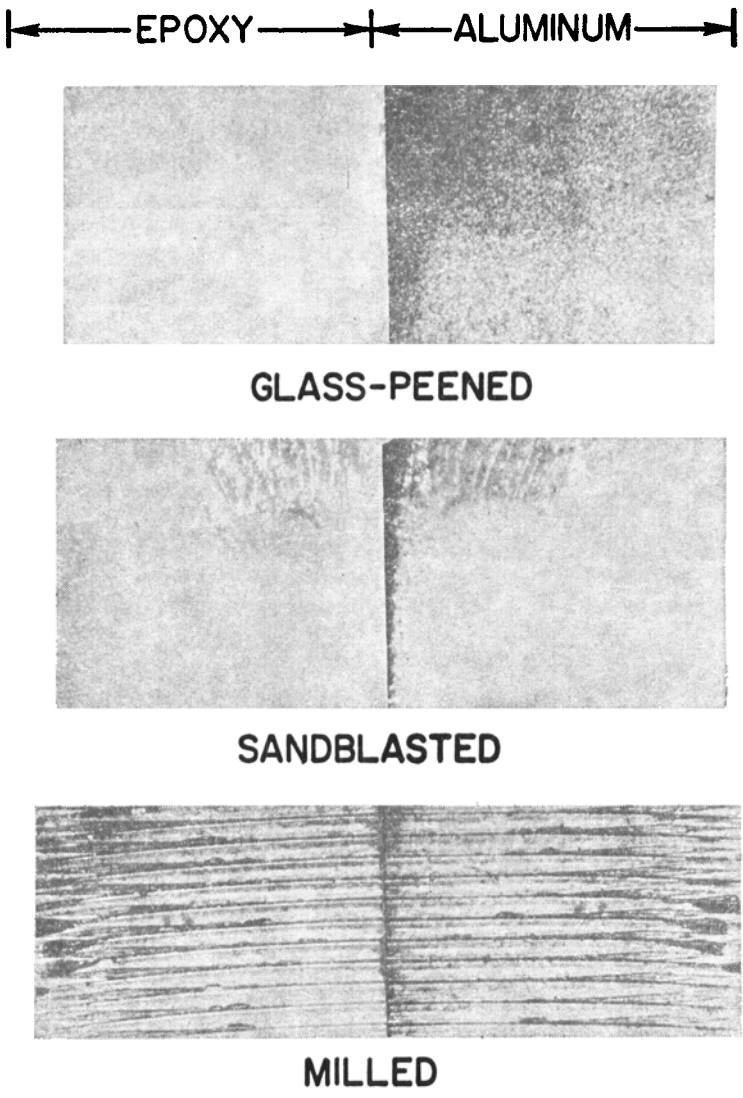

FIGURE 11 Fracture surfaces of epoxy-aluminum specimens with three surface finishes—30×.

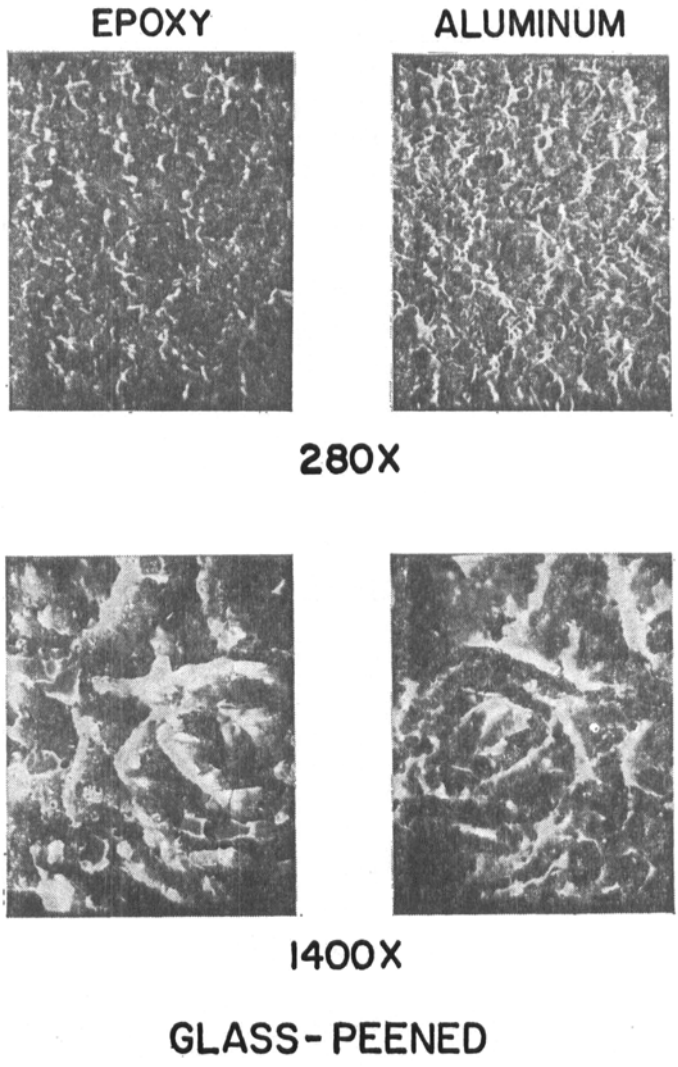

FIGURE 12 Scanning electron microscope photographs of glass-peened epoxy-aluminum fracture surface.

is greater than the roughness on the thickness direction. From fracture surface observations it is apparent that this variation is due to the milling operation, which produces high roughness values in the longitudinal or lengthwise direction but low values in the thickness direction. Roughness measurements in the thickness direction of the milled specimens fall within the range predicted from the relation between surface roughness and strain energy

release rate for the other surface finishes studied. Therefore, the strain energy release rate is dependent on the local surface roughness rather than on gross non-uniformity such as those present in the milled surfaces and its value may be determined from the minimum values of surface roughness over the range considered in this study. Indications from optical observations of the fracture surfaces, Figure 11, show that the crack replicates the surface finish of the aluminum as it propagates along the bond. Based on the relation developed between initial surface roughness and $\mathcal{G}$, greater roughness of fracture surfaces in the epoxy indicate higher strain energy release rates were required for crack propagation. The effect of loading rate or crack velocity on this behaviour was not considered here, although this is an important factor which may affect the failure mode. This result is useful in failure analysis of bonded structures. In many instances the circumstances which caused failure are unknown, and the origin, direction of crack propagation and energy required for crack growth must be determined from observations of the failure surface.

Higher magnification studies using the scanning electron microscope, as shown in Figure 12, indicate that there is a residue of epoxy, which remains bonded to the aluminum surface. These studies also indicate that for stable crack propagation, crack growth occurs very near the interface. Studies conducted by Bascom[21,22] on scarf joints of aluminum bonded with epoxy also indicate that a residue of epoxy remains on the aluminum after interfacial failure. By radioisotope tagging with Carbon-14 he found that a 300 to 500 angstrom layer of resin is left on the aluminum. His fractured specimens also exhibit replication of the scratches and machining marks of the aluminum surface on the resin fracture surface.

CONCLUSION

The purpose of this investigation was to characterize crack propagation at the interface between two dissimilar materials using a formulation based on strain energy release rate and to determine the contribution of the residual stress field to the energy required for crack propagation at an epoxy-aluminum interface. To this end, a theoretical analysis was developed for the plane problem of two elastic half spaces in contact along an arc where one of the materials acts as a relatively rigid body. The stress analysis included the cases of residual stresses, thermal loading and self equilibrating tensile or bending loading applied to either half space. Using this analysis, the elastic strain energy release rate, $\mathcal{G}$, was formulated as a fracture criteria for interfacial failure.

Experimental studies were conducted on specimens of epoxy bonded to

aluminum. In the fabrication of these specimens, the epoxy was cast against the aluminum, and after initial curing, the specimens were post-cured at elevated temperature. This procedure resulted in residual stresses as evidenced by birefringent patterns in the epoxy. The magnitude of the residual stress due to this casting and curing process was determined by photoelastic techniques. Methods were developed for analyzing the birefringent pattern in the epoxy in order to separate the contribution of the elastic residual stress field from that of the frozen stress field. In analyzing interfacial failure of these specimens, knowledge of the magnitude of elastic residual stress field is required, since these stresses contribute to the energy necessary for interfacial crack propagation. As a result of these studies, it was found that elastic residual stresses in this particular geometry combination can contribute 15 to 20% of the strain required for initial crack initiation at the interface.

Following the casting and curing process, cracks were initiated in the epoxy at the interface, and then these specimens were subjected to mechanical loading. The process of interfacial crack propagation was observed, and the data was analyzed using the fracture mechanics formulation derived from the theoretical stress analysis. Results of this analysis indicated that $\mathcal{G}$ can be used to characterize elastic debonding, since the strain energy release rate and crack velocity remained relatively constant as the crack propagated along the bond.

The effect of surface roughness of the aluminum on fracture toughness was measured for four different surface finishes. It was found that increased surface roughness resulted in greater fracture toughness, e.g. sandblast or glass-peen finishes on the aluminum resulted in higher toughness than machined or polished surfaces. This may be explained by the observation that the interfacial cracks replicated the surface fracture of the aluminum. Microscopic studies of the failure surfaces indicate that crack propagation occurs in the epoxy very near the interface, and that a residue of epoxy remains bonded to the aluminum. Therefore, greater surface roughness resulted in greater crack area and higher toughness. This implied that the $\mathcal{G}$ is dependent on the local character of the surface rather than on gross non-uniformity such as those present in the milled specimen. From this data a linear relation was suggested between strain energy release rate and surface roughness over the range of surfaces examined in this study.

The techniques presented in this paper provide a simple method for the study of *interfacial* failure in bonded materials, where one of the materials acts as a relatively rigid body. Results of this investigation have application in design of bonded structures, or in general problems of debonding and delamination between dissimilar bodies. The analysis can be applied to composite materials in analysis of glass-resin interfaces, in bonded joints or

in welded structures where the crack propagates at the interface. This approach can be extended to consider the effects of crack velocity, fatigue loading, environment and various residual fields on the fracture toughness of bonded materials.

Acknowledgements

The authors acknowledge the support of the Office of Naval Research, the Naval Sea Systems Command and the Catholic University of America for the work reported herein, conducted under Project Number RR-023-03-45-5451 and SF 51-544-102-12432.

References

1. M. L. Williams, *Bulletin of the Seismological Society of America* **49,** no. 2, 199–204 (1959).
2. F. Erdogan, *J. of Applied Mechanics, Series E* **30,** no. 2, 232–236 (1963).
3. F. Erdogan, *J. of Applied Mechanics, Series E* **32,** no. 2, 403–410 (1965).
4. A. H. England, *J. of Applied Mechanics, Series E* **32,** no. 2, 400–402 (1965).
5. G. C. Sih and J. R. Rice, *J. of Applied Mechanics, Series E* **31,** no. 3, 477–482 (1964).
6. J. R. Rice and G. C. Sih, *J. of Applied Mechanics, Series E* **32,** no. 2, 418–423 (1965).
7. E. Wu and R. L. Thomas, *Proceedings of the Fifth Int'l Congress on Rheology*, vol. 1 (University Park Press, Baltimore, Md., 1965). Pp. 575–587.
8. C. Wang, "Fracture Mechanics for an Interfacial Crack Between Adhesively Bonded Dissimilar Materials", Dept. of Theoretical and Applied Mechanics, Report No. 353, Univ. of Illinois at Urbana-Champaign, March 1972.
9. M. L. Williams, *J. of Applied Polymer Science* **13,** 29–40 (1969).
10. M. L. Williams, *J. of Applied Polymer Science* **14,** 1121–1126 (1970).
11. M. L. Williams, *J. of Adhesion* **5,** 81 (1973).
12. J. D. Burton, W. B. Jones and M. L. Williams, *Trans. of the Society of Rheology* **15,** 39–50 (1971).
13. S. J. Bennett, K. L. DeVries and M. L. Williams, *International Journal of Fracture* **10,** (1974).
14. D. R. Mulville, "Characteristics of Crack Propagation at the Interface Between Two Dissimilar Media," Doctoral Dissertation, The Catholic University of America, 1974.
15. L. M. Milne-Thomson, *Plane Elastic Systems* (Springer-Verlag, Berlin, 1960).
16. D. R. Mulville, P. W. Mast and R. N. Vaishnav, "Strain Energy Release Rate for Cracks Between Dissimilar Media," Submitted to *Engineering Fracture Mechanics.*
17. N. J. De Lollis, *Adhesives for Metals* (Industrial Press Inc., New York, N.Y., 1970).
18. B. A. Boley and J. H. Weiner, *Theory of Thermal Stress* (J. Wiley and Sons, New York, 1960). Pp. 429–432.
19. A. Durelli, *et al. Mechanics of Composite Systems, Proceedings of 5th Symposium on Naval Structural Mechanics*, J. Wendt *et al.* Eds (Pergamon Press, New York, 1970). pp. 265–336.
20. S. Mostovoy and E. Ripling, *J. Applied Polymer Sci.* **10,** 1351–1371 (1966).
21. W. D. Bascom, "Surface Aspects of Bonding Metals with Polymer Adhesives." Polymer Conference Series on Adhesion, University of Utah, Salt Lake City, Utah, July 1973.
22. W. D. Bascom, et al., *J. of Material Science* **10,** 1037–1048 (1975).